

RESEARCH

Open Access



Enhancing reservoir control in the co-dynamics of HIV-VL: from mathematical modeling perspective

Zinabu Teka Melese¹ and Haileyesus Tessema Alemneh^{2*} 

*Correspondence:

haila.tessema@gmail.com

²Department of Mathematics,
College of Natural and
Computational Sciences, University
of Gondar, Gondar, Ethiopia
Full list of author information is
available at the end of the article

Abstract

HIV patients are vulnerable to developing active visceral leishmaniasis (VL). To understand this complication, we studied a mathematical model for HIV and visceral leishmaniasis coinfection. In this approach, we reckoned two distinct equilibria: the disease-free and the endemic equilibria. The local and global stability of the disease-free equilibrium were thoroughly investigated. To further support the qualitative findings, we performed simulations to quantify the changes of the dynamical behavior of the full model for variation of relevant parameters. Increasing the rate of VL recovery (ϕ_1), the recovery rate for VL–HIV Co-infection (ϕ_2), removing reservoirs (c_1), minimizing the contact rate (β_h) are important in controlling the transmission of individual and co-infection disease of VL and HIV. In conclusion, possible measures should be implemented to reduce the number of infected individuals. Therefore, we recommend that policy makers and stakeholders incorporate these measures during planing and implementation phases to control the transmission of VL–HIV co-infection.

Keywords: VL; HIV; Co-infection; Mathematical model; Stability analysis; Numerical simulation

1 Introduction

Visceral leishmaniasis (VL) also known as ‘Kala-azar’ is a vector borne, zoonotic disease caused by *Leishmania donovani* species [1, 2]. There are more than 20 species of leishmania that can cause human infection. The infection is transmitted following a successful bite and inoculation by the infected phlebotomine female sand flies [3, 4]. The World Health Organization (WHO) considers leishmaniasis as the sixth most important endemic disease in the world [5], and it is distributed around the world in 90 countries [6], most of which are developing countries associated with malnutrition, population displacement, poor housing, a weak immune system, and lack of financial resources [6]. WHO estimated that from about 900,000 to 1.3 million new cases of leishmaniasis are reported per year [1, 2, 6, 7]; of these, approximately 0.2–0.4 million are of visceral leishmaniasis (VL) [6, 7]. The spread of the disease is linked to environmental changes such as deforestation, building of dams, irrigation schemes, and urbanization [7].

© The Author(s) 2021. This article is licensed under a Creative Commons Attribution 4.0 International License, which permits use, sharing, adaptation, distribution and reproduction in any medium or format, as long as you give appropriate credit to the original author(s) and the source, provide a link to the Creative Commons licence, and indicate if changes were made. The images or other third party material in this article are included in the article's Creative Commons licence, unless indicated otherwise in a credit line to the material. If material is not included in the article's Creative Commons licence and your intended use is not permitted by statutory regulation or exceeds the permitted use, you will need to obtain permission directly from the copyright holder. To view a copy of this licence, visit <http://creativecommons.org/licenses/by/4.0/>.

Human immunodeficiency virus (HIV) is the etiological agent responsible for the acquired immunodeficiency syndrome (AIDS) [8]. There are multiple modes of HIV transmission including sexual intercourse, sharing needles with HIV-infected persons, or via HIV-contaminated blood transfusions and others [8]. It is estimated that 36.7 million people worldwide are living with HIV [7] and 2.0 million new infections are reported per year [7, 9]. Also approximately one million died of HIV-related causes globally [10].

It is expected that there is an overlap between the transmission areas of HIV and leishmaniasis. Due to this fact there have been an increasing number of cases of VL–HIV co-infection, which has spread throughout the world [4, 7]. The co-infection has been reported in 35 countries [11, 12]. So that VL–HIV co-infection is an emerging new threat to global public health and development [4, 11, 12].

Mathematical modeling has a great role in describing the dynamics of infectious diseases in a community [13, 14]. Several scholars have developed different models for HIV, VL, and their co-infection with other diseases to study their transmission dynamics. For example, many mathematical models have been developed to understand the transmission nature of HIV [9, 15–18] and VL [19–25] explicitly. In addition, some co-infection models for HIV and malaria [26], HIV-TB [8] and VL and malaria [5] were proposed and analyzed. Hussaini et al. [27] recently presented a mathematical model to study the transmission dynamics of HIV and VL co-infection. In developing their model, they took into account the human and sand fly populations. However, they did not consider the reservoir population for VL and co-infection transmission dynamics in their assumption. Reservoirs are important for maintaining the life cycle of many leishmania species and hence are important for transmission of zoonotic and rural/sylvatic infections. Reservoirs acquire infection with leishmaniasis following contact with infected sand flies, and they are infected to their life time. Treating humans while removing reservoirs from the system reduces the fraction of infected sand flies, which gives a good control strategy against the disease [3, 21].

In this study, we formulated and analyzed mathematical model for VL–HIV co-infection, which incorporates the key epidemiological and biological features of each of the two diseases by considering the reservoir population for VL transmission.

The paper is organized as follows: In Sect. 2, the mathematical model of HIV–VL is presented together with a set of definitions and basic underlying hypotheses. The formulated HIV–VL mathematical model is analyzed in Sect. 3. In Sect. 4 numerical simulations to give a better interpretation of the analytical results were reported. The last part, Sect. 5, is devoted to the discussion and conclusions.

2 Baseline model formulation

In this work, the population that has been considered is classified into three sub-populations, namely the human population, the sand fly population, and the reservoir population; each of them are again divided into different states. The human population $N_h(t)$ that are sexually active in a certain community are sub-divided into susceptible individuals $S_h(t)$, individuals infected with visceral leishmaniasis (VL) only $I_{hl}(t)$, HIV only infected individuals without clinical symptoms of AIDS $I_{hh}(t)$, individuals co-infected with VL and HIV with no clinical symptoms of AIDS $I_{hhl}(t)$, HIV infected individuals with AIDS symptoms $A_h(t)$, and co-infected individuals both with clinical symptoms of AIDS and VL $A_{hl}(t)$.

The number of susceptible individuals can be increased by a constant rate of recruitment Λ_h and recovery from only VL infected class with a rate ϕ_1 and diminished by natural death

Table 1 Parameter descriptions of the HIV–VL co-infection model

Parameter	Description
Λ_h	Recruitment rate of susceptible humans
Λ_s	Recruitment rate of the susceptible sand fly population
Λ_r	Recruitment rate of reservoirs
μ_h	Natural death rate of the human population
μ_s	Natural death rate of the sand fly population
μ_r	Natural death rate of the reservoir population
a_l	Biting rate of sand flies
b_l	VL progression rate in sand flies
c_l	VL progression rate in human and sand fly
ϕ_1, ϕ_2, ϕ_3	Humans recovery rate from VL
δ_l	VL-induced death rate
δ_A	AIDS-induced death rate
β_h	Effective contact rate for HIV infection
κ	HIV progression rate to AIDS stage
$\eta_{hh}, \eta_A, \eta_{hl}$	Modification parameters
$\varepsilon_1, \varepsilon_2, \tau$	Modification parameters

rate μ_h , forces of infection λ_h and λ_l from HIV only and VL only infections, respectively. A susceptible individual can acquire VL infection following the effective contact with VL infected single sand fly at a rate of λ_l , and he/she also acquires HIV at a rate of λ_h if the individual is in effective contact with an HIV infected individual. Once the susceptible individuals are infected with either of infections, they will transfer to the respective infection classes (either $I_{hh}(t)$ or $I_{hl}(t)$). In this co-infection model the natural death rate μ_h is assumed equal for all human population classes. For a more detailed description of the parameters, refer to Table 1. Thus, the total human population is given by

$$N_h(t) = S_h(t) + I_{hl}(t) + I_{hh}(t) + I_{hhl}(t) + A_h(t) + A_{hl}(t).$$

The second sub-population of the model, the sand fly population $N_s(t)$, has two sub-classes denoted by $S_s(t)$ and $I_s(t)$ at time t representing susceptible and infected sand flies, respectively. The susceptible sand flies can be recruited at a rate of Λ_s through birth to the sand fly population. The natural death rate of the sand fly is denoted by μ_s , it can contribute to the reduction of the sand fly susceptible class. This sums the total sand fly population to

$$N_s(t) = S_s(t) + I_s(t).$$

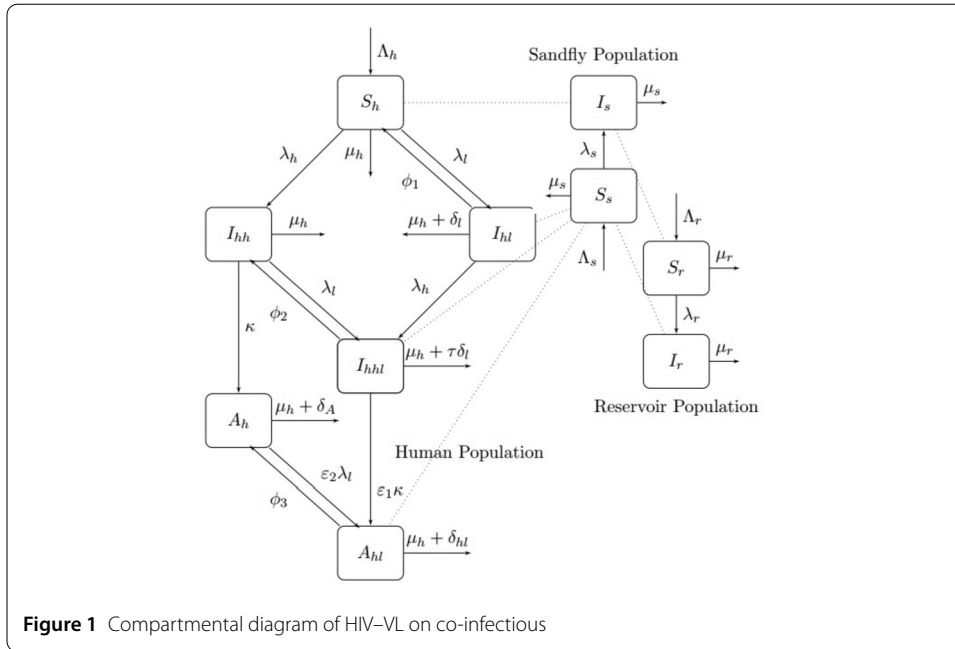
The last sub-population considered in this disease dynamics study is the reservoir population $N_r(t)$ at time t, which is also categorized into two groups; the susceptible class $S_r(t)$ and the infected reservoir $I_r(t)$. Thus, the total reservoir population is given by

$$N_r(t) = S_r(t) + I_r(t).$$

The forces of infection associated with HIV/AIDS, VL, sand flies and reservoir population are denoted by $\lambda_h, \lambda_l, \lambda_s$, and λ_r , respectively, and are given as follows:

$$\lambda_h = \beta_h \left\{ \frac{(I_{hh} + \eta_{hh}I_{hhl}) + \eta_A(A_h + \eta_{hl}A_{hl})}{N_h} \right\},$$

$$\lambda_l = a_l b_l \frac{I_s}{N_h},$$



$$\lambda_s = a_l c_l \left\{ \frac{I_{hl} + I_{hhl} + A_{hl}}{N_h} + \frac{I_r}{N_r} \right\},$$

$$\lambda_r = a_l b_l \frac{I_s}{N_r}.$$

Considering the formulations and assumptions above with the compartmental diagram in Fig. 1, the HIV/AIDS-VL co-infection model can be described by the following system of ordinary differential equations:

$$\begin{aligned} S'_h &= \Lambda_h + \phi_1 I_{hl} - \mu_h S_h - a_l b_l I_s \frac{S_h}{N_h} - \beta_h \left\{ (I_{hh} + \eta_{hh} I_{hhl}) + \eta_A (A_h + \eta_{hl} A_{hl}) \right\} \frac{S_h}{N_h}, \\ I'_{hl} &= a_l b_l I_s \frac{S_h}{N_h} - \beta_h \left\{ (I_{hh} + \eta_{hh} I_{hhl}) + \eta_A (A_h + \eta_{hl} A_{hl}) \right\} \frac{I_{hl}}{N_h} - (\phi_1 + \delta_l + \mu_h) I_{hl}, \\ I'_{hh} &= \beta_h \left\{ (I_{hh} + \eta_{hh} I_{hhl}) + \eta_A (A_h + \eta_{hl} A_{hl}) \right\} \frac{S_h}{N_h} + \phi_2 I_{hhl} - a_l b_l I_s \frac{I_{hh}}{N_h} - (\mu_h + \kappa) I_{hh}, \\ I'_{hhl} &= \beta_h \left\{ (I_{hh} + \eta_{hh} I_{hhl}) + \eta_A (A_h + \eta_{hl} A_{hl}) \right\} \frac{I_{hl}}{N_h} \\ &\quad + a_l b_l I_s \frac{I_{hh}}{N_h} - (\phi_2 + \varepsilon_1 \kappa + \mu_h + \tau \delta_l) I_{hhl}, \\ A'_h &= \kappa I_{hh} + \phi_3 A_{hl} - \varepsilon_2 a_l b_l I_s \frac{A_h}{N_h} - (\delta_A + \mu_h) A_h, \\ A'_{hl} &= \varepsilon_1 \kappa I_{hhl} + \varepsilon_2 a_l b_l I_s \frac{A_h}{N_h} - (\phi_3 + \delta_{hl} + \mu_h) A_{hl}, \\ S'_s &= \Lambda_s - a_l c_l \left(\frac{I_{hl} + I_{hhl} + A_{hl}}{N_h} + \frac{I_r}{N_r} \right) S_s - \mu_s S_s, \\ I'_s &= a_l c_l \left(\frac{I_{hl} + I_{hhl} + A_{hl}}{N_h} + \frac{I_r}{N_r} \right) S_s - \mu_s I_s, \end{aligned} \tag{1}$$

$$S'_r = \Lambda_r - a_l b_l I_s \frac{S_r}{N_r} - \mu_r S_r,$$

$$I'_r = a_l b_l I_s \frac{S_r}{N_r} - \mu_r I_r.$$

The rates of change for the total human population, the sand fly population, and the reservoir population with change in time are as follows:

$$N'_h = \Lambda_h - \mu_h N_h - (\delta_l I_{hl} + \tau \delta_l I_{hhl} + \delta_A A_h + \delta_{hl} A_{hl}),$$

$$N'_s = \Lambda_s - \mu_s N_s,$$

$$N'_r = \Lambda_r - \mu_r N_r,$$

where $\phi_2 = \iota_1 \phi_1$, $\phi_3 = \iota_2 \phi_1$, $\delta_{hl} = \epsilon \delta_A + \tau \delta_l$.

2.1 Invariant region

The system in (1) describes the epidemiological dynamics of the human population, the sand fly population, and the reservoir population. If disease specific induced death rates are assumed negligible ($\delta_l = 0 = \delta_A = \delta_{hl}$), then

$$\limsup_{t \rightarrow \infty} N_h(t) = \frac{\Lambda_h}{\mu_h}, \quad \limsup_{t \rightarrow \infty} N_s(t) = \frac{\Lambda_s}{\mu_s}, \quad \text{and} \quad \limsup_{t \rightarrow \infty} N_r(t) = \frac{\Lambda_r}{\mu_r}.$$

Thus, the feasible region is

$$\Omega = \left\{ (S_h, I_{hl}, I_{hh}, I_{hhl}, A_h, A_{hl}, S_s, I_s, S_r, I_r) \in \mathbb{R}_+^{10} : S_h, I_{hl}, I_{hh}, I_{hhl}, A_h, A_{hl}, S_s, I_s, S_r, I_r \geq 0, N_h \leq \frac{\Lambda_h}{\mu_h}, N_s \leq \frac{\Lambda_s}{\mu_s}, N_r \leq \frac{\Lambda_r}{\mu_r} \right\}.$$

All the model parameters and variables are nonnegative. If nonnegative initial values of the state variables are taken from this region, then the solution of system (1) will remain in Ω . Therefore, this region is a positively invariant set, and hence studying the dynamics of model (1) in the biologically meaningful and mathematically well-posed region Ω is sufficient.

3 Analysis of the HIV/AIDS–VL co-infection model

Model analysis is an important part in modeling the epidemiological phenomenon to find the qualitative and theoretical results. Before proceeding to further analysis, nondimensionalizing the sub-populations as seen below helps to study the proportion of each of the state variables.

$$\begin{aligned} s_h(t) &= \frac{S_h(t)}{N_h(t)}, & i_{hl}(t) &= \frac{I_{hl}(t)}{N_h(t)}, & i_{hh}(t) &= \frac{I_{hh}(t)}{N_h(t)}, \\ i_{hhl}(t) &= \frac{I_{hhl}(t)}{N_h(t)}, & a_h(t) &= \frac{A_h(t)}{N_h(t)}, \\ a_{hl}(t) &= \frac{A_{hl}(t)}{N_h(t)}, & s_s(t) &= \frac{S_s(t)}{N_s(t)}, & i_s(t) &= \frac{I_s(t)}{N_s(t)}, \end{aligned}$$

$$s_r(t) = \frac{S_r(t)}{N_r(t)}, \quad i_r(t) = \frac{I_r(t)}{N_r(t)}.$$

Here, it can be defined that $p = \frac{N_s}{N_h}$ and $q = \frac{N_s}{N_r}$ are the female sand fly–human ratio and female sand fly–reservoir ratio [5], respectively, and they can be assumed as constants [28]. Then the new deterministic model for the above re-scaled classes is as follows:

$$\begin{aligned} s'_h &= \frac{\Lambda_h}{N_h} + \phi_1 i_{hl} - a_1 b_1 p i_s s_h - \beta_h \{ (i_{hh} + \eta_{hh} i_{hhl}) + \eta_A (a_h + \eta_{hl} a_{hl}) \} s_h \\ &\quad - \left(\frac{\Lambda_h}{N_h} - (\delta_1 i_{hl} + \tau \delta_1 i_{hhl} + \delta_A a_h + \delta_{hl} a_{hl}) \right) s_h, \\ i'_{hl} &= a_1 b_1 p i_s s_h - \beta_h \{ (i_{hh} + \eta_{hh} i_{hhl}) + \eta_A (a_h + \eta_{hl} a_{hl}) \} i_{hl} - \phi_1 i_{hl} \\ &\quad - \left(\frac{\Lambda_h}{N_h} + \delta_l - (\delta_1 i_{hl} + \tau \delta_1 i_{hhl} + \delta_A a_h + \delta_{hl} a_{hl}) \right) i_{hl}, \\ i'_{hh} &= \beta_h \{ (i_{hh} + \eta_{hh} i_{hhl}) + \eta_A (a_h + \eta_{hl} a_{hl}) \} s_h + \phi_2 i_{hhl} - a_1 b_1 p i_s i_{hh} \\ &\quad - \kappa i_{hh} - \left(\frac{\Lambda_h}{N_h} - (\delta_1 i_{hl} + \tau \delta_1 i_{hhl} + \delta_A a_h + \delta_{hl} a_{hl}) \right) i_{hh}, \\ i'_{hhl} &= \beta_h \{ (i_{hh} + \eta_{hh} i_{hhl}) + \eta_A (a_h + \eta_{hl} a_{hl}) \} i_{hl} + a_1 b_1 p i_s i_{hh} \\ &\quad - \left(\frac{\Lambda_h}{N_h} + \phi_2 + \varepsilon_1 \kappa + \tau \delta_l - (\delta_1 i_{hl} + \tau \delta_1 i_{hhl} + \delta_A a_h + \delta_{hl} a_{hl}) \right) i_{hhl}, \\ a'_h &= \kappa i_{hh} + \phi_3 a_{hl} - \varepsilon_2 a_1 b_1 p i_s a_h - \left(\frac{\Lambda_h}{N_h} + \delta_A - (\delta_1 i_{hl} + \tau \delta_1 i_{hhl} + \delta_A a_h + \delta_{hl} a_{hl}) \right) a_h, \\ a'_{hl} &= \varepsilon_1 \kappa i_{hhl} + \varepsilon_2 a_1 b_1 p i_s a_h - \left(\frac{\Lambda_h}{N_h} + \phi_3 + \delta_{hl} - (\delta_1 i_{hl} + \tau \delta_1 i_{hhl} + \delta_A a_h + \delta_{hl} a_{hl}) \right) a_{hl}, \\ s'_s &= \frac{\Lambda_s}{N_s} - a_1 c_l (i_{hl} + i_{hhl} + a_{hl} + i_r) s_s - \frac{\Lambda_s}{N_s} s_s, \\ i'_s &= a_1 c_l (i_{hl} + i_{hhl} + a_{hl} + i_r) s_s - \frac{\Lambda_s}{N_s} i_s, \\ s'_r &= \frac{\Lambda_r}{N_r} - a_1 b_1 q i_s s_r - \frac{\Lambda_r}{N_r} s_r, \\ i'_r &= a_1 b_1 q i_s s_r - \frac{\Lambda_r}{N_r} i_r \end{aligned} \tag{2}$$

with the biologically feasible region of

$$\begin{aligned} \Phi &= \{ (s_h, i_{hl}, i_{hh}, i_{hhl}, a_h, a_{hl}, s_s, i_s, s_r, i_r) \in \mathbb{R}_+^{10} : 0 \leq s_h, i_{hl}, i_{hh}, i_{hhl}, \\ &\quad a_h, a_{hl} \leq 1, 0 \leq s_s, i_s \leq 1, 0 \leq s_r, i_r \leq 1 \}. \end{aligned}$$

Region Φ is a positively invariant domain, and it is mathematically well-posed under system (2). Now it is possible to proceed to the detailed analysis of epidemiological model (2).

3.1 Disease-free equilibrium and basic reproduction number

Studying the possibility of the population to be invaded has paramount importance. Here the disease-free state that shows the absence of the diseases is investigated. The DFE for

system (2) is given by

$$\mathcal{E}_0 = (s_h^*, i_{hl}^*, i_{hh}^*, i_{hh}^*, a_h^*, a_{hl}^*, s_s^*, i_s^*, s_r^*, i_r^*) = (1, 0, 0, 0, 0, 0, 1, 0, 1, 0).$$

Using the next generation approach (see [29, 30]), \mathcal{F} and \mathcal{V} stand for new infections and transition of infection rates, respectively. The partial derivatives of \mathcal{F} and \mathcal{V} with respect to each non-susceptible class are denoted by F and V , respectively, where

$$F = \begin{pmatrix} 0 & 0 & 0 & 0 & 0 & a_l b_l p & 0 \\ 0 & \beta_h & \beta_h \eta_{hl} & \beta_h \eta_A & \beta_h \eta_A \eta_{hl} & 0 & 0 \\ 0 & 0 & 0 & 0 & 0 & 0 & 0 \\ 0 & 0 & 0 & 0 & 0 & 0 & 0 \\ 0 & 0 & 0 & 0 & 0 & 0 & 0 \\ a_l c_l & 0 & a_l c_l & 0 & a_l c_l & 0 & a_l c_l \\ 0 & 0 & 0 & 0 & 0 & a_l b_l q & 0 \end{pmatrix}$$

and

$$V = \begin{pmatrix} v_{11} & 0 & 0 & 0 & 0 & 0 & 0 \\ 0 & v_{22} & -\phi_2 & 0 & 0 & 0 & 0 \\ 0 & 0 & v_{33} & 0 & 0 & 0 & 0 \\ 0 & -\kappa & 0 & v_{44} & -\phi_3 & 0 & 0 \\ 0 & 0 & -\varepsilon_1 \kappa & 0 & v_{55} & 0 & 0 \\ 0 & 0 & 0 & 0 & 0 & \mu_s & 0 \\ 0 & 0 & 0 & 0 & 0 & 0 & \mu_r \end{pmatrix},$$

where $v_{11} = \phi_1 + \delta_l + \mu_h$, $v_{22} = \kappa + \mu_h$, $v_{33} = \phi_2 + \varepsilon_1 \kappa + \tau \delta_l + \mu_h$, $v_{44} = \delta_A + \mu_h$, $v_{55} = \phi_3 + \delta_{hl} + \mu_h$.

Then the basic reproduction number associated with system (2) is defined by the spectral radius of the next generation matrix FV^{-1} and obtained as

$$\mathcal{R}_0 = \max \left\{ \frac{\beta_h(\delta_A + \mu_h + \eta_A \kappa)}{(\kappa + \mu_h)(\delta_A + \mu_h)}, \sqrt{\frac{a_l c_l(\mu_r a_l b_l p + a_l b_l q(\phi_1 + \delta_l + \mu_h))}{\mu_s \mu_r(\phi_1 + \delta_l + \mu_h)}} \right\}.$$

Furthermore, it can also be given as $\mathcal{R}_0 = \rho(FV^{-1}) = \max\{\mathcal{R}_{0h}, \mathcal{R}_{0l}\}$.

$\mathcal{R}_{0l} = \frac{\beta_h(\delta_A + \mu_h + \eta_A \kappa)}{(\kappa + \mu_h)(\delta_A + \mu_h)}$ is the basic reproduction number for an HIV only model, i.e., at the absence of VL. And $\mathcal{R}_{0h} = \sqrt{\frac{a_l c_l(\mu_r a_l b_l p + a_l b_l q(\phi_1 + \delta_l + \mu_h))}{\mu_s \mu_r(\phi_1 + \delta_l + \mu_h)}}$ represents the reproduction number for a VL only model at the absence of HIV.

Theorem 3.1 *The DFE of system (2) \mathcal{E}_0 is locally asymptotically stable in Φ if $\mathcal{R}_0 < 1$ and unstable if $\mathcal{R}_0 > 1$.*

Proof To prove Theorem 3.1, it is apparent to start with linearizing model (2) around \mathcal{E}_0 . Thus, the Jacobian matrix is given as follows:

$$J_{\mathcal{E}_0} = \begin{pmatrix} -\mu_h & j_{12} & -\beta_h & j_{14} & j_{15} & j_{16} & 0 & -a_l b_l p & 0 & 0 \\ 0 & -j_{22} & 0 & 0 & 0 & 0 & 0 & a_l b_l p & 0 & 0 \\ 0 & 0 & j_{33} & j_{34} & \beta_h \eta_A & \beta_h \eta_A \eta_{hl} & 0 & 0 & 0 & 0 \\ 0 & 0 & 0 & -j_{44} & 0 & 0 & 0 & 0 & 0 & 0 \\ 0 & 0 & \kappa & 0 & -j_{55} & \phi_3 & 0 & 0 & 0 & 0 \\ 0 & 0 & 0 & \varepsilon_1 \kappa & 0 & -j_{66} & 0 & 0 & 0 & 0 \\ 0 & -a_l c_l & 0 & -a_l c_l & 0 & -a_l c_l & -\mu_s & 0 & 0 & -a_l c_l \\ 0 & a_l c_l & 0 & a_l c_l & 0 & a_l c_l & 0 & -\mu_s & 0 & a_l c_l \\ 0 & 0 & 0 & 0 & 0 & 0 & 0 & -a_l b_l q & -\mu_r & 0 \\ 0 & 0 & 0 & 0 & 0 & 0 & 0 & a_l b_l q & 0 & -\mu_r \end{pmatrix},$$

where $j_{12} = \phi_1 + \delta_l, j_{14} = -\beta_h \eta_{hh} + \tau \delta_l, j_{15} = -\beta_h \eta_A + \delta_A, j_{16} = -\beta_h \eta_A \eta_{hl} + \delta_{hl}, j_{22} = \phi_1 + \delta_l + \mu_h, j_{33} = \beta_h - \kappa - \mu_h, j_{34} = \beta_h \eta_{hh} + \phi_2, j_{44} = \phi_2 + \varepsilon_1 \kappa + \tau \delta_l + \mu_h, j_{55} = \delta_A + \mu_h, j_{66} = \phi_3 + \delta_{hl} + \mu_h$.

Hence the eigenvalues of the matrix $J_{\mathcal{E}_0}$ are $\lambda_1 = -\mu_h, \lambda_4 = -(\phi_2 + \varepsilon_1 \kappa + \tau \delta_l + \mu_h), \lambda_6 = -(\phi_3 + \delta_{hl} + \mu_h), \lambda_7 = -\mu_s, \lambda_9 = -\mu_r$, and the rest can be obtained from the following characteristic polynomials:

$$\begin{aligned} \lambda^2 + A_1 \lambda + A_0 &= 0, \\ \lambda^3 + B_2 \lambda^2 + B_1 \lambda + B_0 &= 0, \end{aligned} \tag{3}$$

where $A_1 = \kappa + \delta_A + 2\mu_h - \beta_h, A_0 = -\beta_h \eta_A \kappa - (\beta_h - \kappa - \mu_h)(\delta_A + \mu_h), B_2 = \mu_r + \mu_s + \mu_h + \phi_2 + \delta_l, B_1 = (\mu_h + \phi_2 + \delta_l)(\mu_r + \mu_s) + \mu_r \mu_s - a_l c_l a_l b_l q - a_l c_l p a_l b_l, B_0 = (\mu_h + \phi_2 + \delta_l)(\mu_r \mu_s - a_l c_l a_l b_l q) - a_l b_l p a_l c_l \mu_r$.

For a quadratic polynomial to have negative roots, the Routh–Hurwitz stability criterion states that both A_1 and A_0 must be greater than zero. Thus, from the quadratic equation of system (3) if $\mathcal{R}_0 < 1, A_1$ and A_0 yield

$$\begin{aligned} \kappa + \delta_A + 2\mu_h &> \beta_h, \\ -\beta_h \eta_A \kappa - (\beta_h - \kappa - \mu_h)(\delta_A + \mu_h) &> 0 \implies \mathcal{R}_0 < 1. \end{aligned}$$

And for cubic polynomial the criterion is $B_2 > 0, B_0 > 0$ and $B_2 B_1 - B_0 > 0$. Thus, from the cubic polynomial of equation (3), B_2 is apparently positive; as can be seen it is the sum of positive parameters. It is given for $B_0 > 0$ that

$$(\mu_h + \phi_2 + \delta_l)(\mu_r \mu_s - a_l c_l a_l b_l q) - a_l b_l p a_l c_l \mu_r > 0,$$

which simplified to $\mathcal{R}_0 < 1$. And for $B_2 B_1 - B_0 > 0$,

$$\begin{aligned} (\mu_r + \mu_s + \mu_h + \phi_2 + \delta_l)((\mu_h + \phi_2 + \delta_l)(\mu_r + \mu_s) + \mu_r \mu_s - a_l c_l a_l b_l q - a_l c_l p a_l b_l) \\ - (\mu_h + \phi_2 + \delta_l)(\mu_r \mu_s - a_l c_l a_l b_l q) + a_l b_l p a_l c_l \mu_r > 0 \end{aligned}$$

also holds. Therefore, whenever $\mathcal{R}_0 < 1$, the DFE becomes locally asymptotically stable. \square

3.1.1 Global stability of DFE

Applying the Castillo–Chavez et al. [31] (Appendix A), let us rewrite the model in system (2) as

$$\begin{aligned} \frac{dX}{dt} &= F(X, Z), \\ \frac{dZ}{dt} &= G(X, Z), G(X, 0) = 0. \end{aligned}$$

The column vector X contains uninfected classes, while the components of vector Z are the infected individuals. Thus, for the transformed system, model (2) is

$$\begin{aligned} X &= (s_h, s_s, s_r), \\ Z &= (i_{hl}, i_{hh}, i_{hhl}, a_h, a_{hl}). \end{aligned}$$

From the first condition, $\frac{dX}{dt} = F(X, 0)$, X^* is globally asymptotically stable, the reduced system is given by

$$F(X, 0) = \begin{pmatrix} \frac{\Lambda_h}{N_h} - \mu_h s_h \\ \frac{\Lambda_s}{N_s} - \mu_s s_s \\ \frac{\Lambda_r}{N_r} - \mu_r s_r \end{pmatrix}.$$

Therefore, for the DFE of system (2), say $E_0 = (X^*, 0)$, to be globally stable, the following two conditions must be satisfied [31]. From the second condition, $G(X, Z) = \mathcal{A}Z - \hat{G}(X, Z)$ with $\hat{G}(X, Z) \geq 0$, where $\mathcal{A} = D_z G(X^*, 0) = (\frac{\partial G_i}{\partial z_j}(X^*, 0))$ is the linearization matrix of system (2) evaluated at E_0 . Hence, the matrix \mathcal{A} is

$$\mathcal{A} = \begin{pmatrix} -v_{11} & 0 & 0 & 0 & 0 & a_1 b_1 p & 0 \\ 0 & v_{22} & \beta_h \eta_{hl} + \phi_2 & \beta_h \eta_A & \beta_h \eta_A \eta_{hl} & 0 & 0 \\ 0 & 0 & -v_{33} & 0 & 0 & 0 & 0 \\ 0 & \kappa & 0 & -v_{44} & \phi_3 & 0 & 0 \\ 0 & 0 & \varepsilon_1 \kappa & 0 & -v_{55} & 0 & 0 \\ a_1 c_l & 0 & a_1 c_l & 0 & a_1 c_l & -\mu_s & a_1 c_l \\ 0 & 0 & 0 & 0 & 0 & a_1 b_1 q & -\mu_r \end{pmatrix},$$

where only v_{22} is changed to $\beta_h - \kappa - \mu_h$, the rest are as defined previously. Now the column vector $\hat{G}(X, Z)$ is given by

$$\begin{aligned} \hat{G}(X, Z) &= \begin{pmatrix} \hat{G}_1(X, Z) \\ \hat{G}_2(X, Z) \\ \hat{G}_3(X, Z) \\ \hat{G}_4(X, Z) \\ \hat{G}_5(X, Z) \end{pmatrix} \\ &= \begin{pmatrix} a_1 b_1 p i_s (1 - s_h) + \beta_h (i_{hh} + \eta_{hl} i_{hl} + \eta_A (a_h + \eta_{hl})) i_{hl} \\ \beta_h (i_{hh} + \eta_{hl} i_{hl} + \eta_A (a_h + \eta_{hl})) (1 - s_h) + a_1 b_1 p i_s i_{hh} \\ - (\beta_h (i_{hh} + \eta_{hl} i_{hl} + \eta_A (a_h + \eta_{hl})) i_{hl} + a_1 b_1 p i_s i_{hh}) \\ \varepsilon_1 a_1 b_1 p i_s a_h \\ - \varepsilon_1 a_1 b_1 p i_s a_h a_1 c_l (i_{hl} + i_{hhl} + a_{hl} + i_r) (1 - s_s) a_1 b_1 q i_s (1 - s_r) \end{pmatrix} \end{aligned} \tag{4}$$

This implied that the third and the fifth entries of $\hat{G}(X, Z)$ are negative if all the parameters and the state variables in those entries are taken strictly positive. Hence $\hat{G}(X, Z)$ is not greater than zero. Thus, the second condition (H_2) stated above is not fulfilled. This concludes that the DFE may not be globally asymptotically stable. Apart from the following special cases, this may be a guarantee for bifurcation analysis. For two special cases, we have the following sub-results.

Lemma 3.2

- (a) *The DFE of system (2) \mathcal{E}_0 is globally asymptotically stable if HIV/AIDS patients are protected against VL whenever there is maximum protection against HIV/AIDS ($\beta_h = 0$).*
- (b) *The DFE of system (2) \mathcal{E}_0 is globally asymptotically stable if VL patients are protected against HIV/AIDS whenever there is maximum protection against VL ($a_l = 0$).*

3.2 Bifurcation analysis

The center manifold theory [31–35], particularly we use the theorem in Castillo–Chavez and Song [31] (Appendix A), helps to study the possibility of backward bifurcation. To determine the direction of bifurcation of system (2) through applying this theory, initially the variables are renamed as $x_1 = s_h, x_2 = i_{hl}, x_3 = i_{hh}, x_4 = i_{hhl}, x_5 = a_h, x_6 = a_{hl}, x_7 = s_s, x_8 = i_s, x_9 = s_r, x_{10} = i_r$ with vector representation of $\mathbf{x} = (x_1, x_2, x_3, x_4, x_5, x_6, x_7, x_8, x_9, x_{10})^T$. If the model is denoted by $\mathbf{x}' = \mathbf{f}(\mathbf{x})$ with $\mathbf{f}(\mathbf{x}) = (f_1(\mathbf{x}), f_2(\mathbf{x}), f_3(\mathbf{x}), f_4(\mathbf{x}), f_5(\mathbf{x}), f_6(\mathbf{x}), f_7(\mathbf{x}), f_8(\mathbf{x}), f_9(\mathbf{x}), f_{10}(\mathbf{x}))^T$, then system (2) can be rewritten as follows:

$$\begin{aligned}
 x'_1 = f_1 &= \frac{\Lambda_h}{N_h} + \phi_1 x_2 - a_l b_l p x_8 x_1 - \beta_h \{ (x_3 + \eta_{hh} x_4) + \eta_A (x_5 + \eta_{hl} x_6) \} x_1 \\
 &\quad - \left(\frac{\Lambda_h}{N_h} - (\delta_l x_2 + \tau \delta_l x_4 + \delta_A x_5 + \delta_{hl} x_6) \right) x_1, \\
 x'_2 = f_2 &= a_l b_l p x_8 x_1 - \beta_h \{ (x_3 + \eta_{hh} x_4) + \eta_A (x_5 + \eta_{hl} x_6) \} x_2 - \phi_1 x_2 \\
 &\quad - \left(\frac{\Lambda_h}{N_h} + \delta_l - (\delta_l x_2 + \tau \delta_l x_4 + \delta_A x_5 + \delta_{hl} x_6) \right) x_2, \\
 x'_3 = f_3 &= \beta_h \{ (x_3 + \eta_{hh} x_4) + \eta_A (x_5 + \eta_{hl} x_6) \} x_1 + \phi_2 x_4 - a_l b_l p x_8 x_3 \\
 &\quad - \kappa x_3 - \left(\frac{\Lambda_h}{N_h} - (\delta_l x_2 + \tau \delta_l x_4 + \delta_A x_5 + \delta_{hl} x_6) \right) x_3, \\
 x'_4 = f_4 &= \beta_h \{ (x_3 + \eta_{hh} x_4) + \eta_A (x_5 + \eta_{hl} x_6) \} x_2 + a_l b_l p x_8 x_3 \\
 &\quad - \left(\frac{\Lambda_h}{N_h} + \phi_2 + \varepsilon_1 \kappa + \tau \delta_l - (\delta_l x_2 + \tau \delta_l x_4 + \delta_A x_5 + \delta_{hl} x_6) \right) x_4, \\
 x'_5 = f_5 &= \kappa x_3 + \phi_3 x_6 - \varepsilon_2 a_l b_l p x_8 x_5 - \left(\frac{\Lambda_h}{N_h} + \delta_A - (\delta_l x_2 + \tau \delta_l x_4 + \delta_A x_5 + \delta_{hl} x_6) \right) x_5, \\
 x'_6 = f_6 &= \varepsilon_1 \kappa x_4 + \varepsilon_2 a_l b_l p x_8 x_5 \\
 &\quad - \left(\frac{\Lambda_h}{N_h} + \phi_3 + \delta_{hl} - (\delta_l x_2 + \tau \delta_l x_4 + \delta_A x_5 + \delta_{hl} x_6) \right) x_6, \\
 x'_7 = f_7 &= \frac{\Lambda_s}{N_s} - a_l c_l (x_2 + x_4 + x_6 + x_{10}) x_7 - \frac{\Lambda_s}{N_s} x_7,
 \end{aligned}
 \tag{5}$$

$$\begin{aligned}
 x'_8 = f_8 &= a_1c_l(x_2 + x_4 + x_6 + x_{10})x_7 - \frac{\Lambda_s}{N_s}x_8, \\
 x'_9 = f_9 &= \frac{\Lambda_r}{N_r} - a_1b_lqx_8x_9 - \frac{\Lambda_r}{N_r}x_9, \\
 x'_{10} = f_{10} &= a_1b_lqx_8x_9 - \frac{\Lambda_r}{N_r}x_{10}.
 \end{aligned}$$

Let $\beta_h = \beta^* = \frac{(\kappa + \mu_h)(\delta_A + \mu_h)}{\delta_A + \mu_h + \eta_A \kappa}$ be the bifurcation parameter solved at $\mathcal{R}_{0l} < \mathcal{R}_{0h} = 1$ ($\mathcal{R}_0 = 1$). Then the Jacobian of system (5) at DFE is given by

$$J_{\beta^*} = \begin{pmatrix} -\mu_h & j_{12} & -\beta^* & j_{14} & j_{15} & j_{16} & 0 & -a_1b_l p & 0 & 0 \\ 0 & -j_{22} & 0 & 0 & 0 & 0 & 0 & a_1b_l p & 0 & 0 \\ 0 & 0 & j_{33} & j_{34} & \beta^* \eta_A & \beta^* \eta_A \eta_{hl} & 0 & 0 & 0 & 0 \\ 0 & 0 & 0 & -j_{44} & 0 & 0 & 0 & 0 & 0 & 0 \\ 0 & 0 & \kappa & 0 & -j_{55} & \phi_3 & 0 & 0 & 0 & 0 \\ 0 & 0 & 0 & \varepsilon_1 \kappa & 0 & -j_{66} & 0 & 0 & 0 & 0 \\ 0 & -a_1c_l & 0 & -a_1c_l & 0 & -a_1c_l & -\mu_s & 0 & 0 & -a_1c_l \\ 0 & a_1c_l & 0 & a_1c_l & 0 & a_1c_l & 0 & -\mu_s & 0 & a_1c_l \\ 0 & 0 & 0 & 0 & 0 & 0 & 0 & -a_1b_l q & -\mu_r & 0 \\ 0 & 0 & 0 & 0 & 0 & 0 & 0 & a_1b_l q & 0 & -\mu_r \end{pmatrix},$$

where the shorthand representations are as given previously, but β_h is given by the bifurcation parameter β^* . There are two eigenvectors associated with J_{β^*} at its simple (zero) eigenvalue. Thus, the right eigenvector denoted by $(\mathbf{w} = (w_1, w_2, w_3, w_4, w_5, w_6, w_7, w_8, w_9, w_{10})^T)$ has the entries as given below.

$$\begin{aligned}
 w_1 &= \frac{j_{12}w_2 - \beta^*w_3 + j_{15}w_5 - a_1b_l w_8}{\mu_h}, & w_2 &= \frac{a_1b_l p w_8}{j_{22}}, & w_3 &= \frac{j_{55}w_5}{\kappa}, \\
 w_4 &= 0, & w_5 &= w_5, & w_6 &= 0, & w_7 &= -w_8, \\
 w_8 &= w_8, & w_9 &= -w_{10}, & w_{10} &= w_{10}.
 \end{aligned} \tag{6}$$

And the left eigenvector represented by $(\mathbf{v} = (v_1, v_2, v_3, v_4, v_5, v_6, v_7, v_8, v_9, v_{10})^T)$ is given with the following values of entries:

$$\begin{aligned}
 v_1 &= 0, & v_2 &= \frac{a_1c_l v_8}{j_{22}}, & v_3 &= \frac{-\kappa v_5}{j_{33}}, \\
 v_4 &= \frac{\varepsilon_1 \kappa v_6 + j_{34}v_3 + a_1c_l v_8}{j_{44}}, & v_5 &= v_5, \\
 v_6 &= \frac{\beta^* \eta_A \eta_{hl} v_3 + \phi_3 v_5 + a_1c_l v_8}{j_{66}}, & v_7 &= 0, \\
 v_8 &= \frac{\mu_r v_{10}}{a_1c_l}, & v_9 &= 0, & v_{10} &= v_{10}.
 \end{aligned} \tag{7}$$

The center manifold approach described in [31] is used to study the direction of bifurcation analysis with computation of a and b, where

$$a = \sum_{k,i,j=1}^{10} v_k w_i w_j \frac{\partial f_k}{\partial x_i \partial x_j} (\mathcal{E}_0, \beta^*)$$

$$b = \sum_{k,i=1}^{10} v_k w_i \frac{\partial f_k}{\partial x_i \partial \beta_h} (\mathcal{E}_0, \beta^*).$$

The first, the seventh, and the ninth entries of the left eigenvector are zero, thus the partial derivatives of the corresponding drift functions ($f_1, f_7,$ and f_9) are not important in computing a and b than wasting time. Thus, from system (5), the only crucial ones and nonzero derivative of the drift evaluated at (\mathcal{E}_0, β^*) are given below.

$$\begin{aligned} \frac{\partial^2 f_2}{\partial x_2 \partial x_3} &= \frac{\partial^2 f_2}{\partial x_3 \partial x_2} = -\beta^*, & \frac{\partial^2 f_2}{\partial x_2 \partial x_4} &= \frac{\partial^2 f_2}{\partial x_4 \partial x_2} = -\beta^* \eta_{hh}, \\ \frac{\partial^2 f_2}{\partial x_2 \partial x_5} &= \frac{\partial^2 f_2}{\partial x_5 \partial x_2} = -\beta^* \eta_A, & \frac{\partial^2 f_2}{\partial x_2 \partial x_6} &= \frac{\partial^2 f_2}{\partial x_6 \partial x_2} = -\beta^* \eta_A \eta_{hl}, \\ \frac{\partial^2 f_2}{\partial x_1 \partial x_8} &= \frac{\partial^2 f_2}{\partial x_8 \partial x_1} = a_1 b_1 p, \\ \frac{\partial^2 f_3}{\partial x_1 \partial x_3} &= \frac{\partial^2 f_3}{\partial x_3 \partial x_1} = \beta^*, & \frac{\partial^2 f_3}{\partial x_1 \partial x_4} &= \frac{\partial^2 f_3}{\partial x_4 \partial x_1} = \beta^* \eta_{hh}, \\ \frac{\partial^2 f_3}{\partial x_1 \partial x_5} &= \frac{\partial^2 f_3}{\partial x_5 \partial x_1} = \beta^* \eta_A, & \frac{\partial^2 f_3}{\partial x_1 \partial x_6} &= \frac{\partial^2 f_3}{\partial x_6 \partial x_1} = \beta^* \eta_A \eta_{hl}, \\ \frac{\partial^2 f_3}{\partial x_3 \partial x_8} &= \frac{\partial^2 f_3}{\partial x_8 \partial x_3} = -a_1 b_1 p, \\ \frac{\partial^2 f_4}{\partial x_2 \partial x_3} &= \frac{\partial^2 f_4}{\partial x_3 \partial x_2} = \beta^*, & \frac{\partial^2 f_4}{\partial x_2 \partial x_4} &= \frac{\partial^2 f_4}{\partial x_4 \partial x_2} = \beta^* \eta_{hh}, \\ \frac{\partial^2 f_4}{\partial x_2 \partial x_5} &= \frac{\partial^2 f_4}{\partial x_5 \partial x_2} = \beta^* \eta_A, & \frac{\partial^2 f_4}{\partial x_2 \partial x_6} &= \frac{\partial^2 f_4}{\partial x_6 \partial x_2} = \beta^* \eta_A \eta_{hl}, \\ \frac{\partial^2 f_4}{\partial x_3 \partial x_8} &= \frac{\partial^2 f_4}{\partial x_8 \partial x_3} = a_1 b_1 p, \\ \frac{\partial^2 f_5}{\partial x_5 \partial x_8} &= \frac{\partial^2 f_5}{\partial x_8 \partial x_5} = -\varepsilon_2 a_1 b_1 p, & \frac{\partial^2 f_6}{\partial x_5 \partial x_8} &= \frac{\partial^2 f_6}{\partial x_8 \partial x_5} = \varepsilon_2 a_1 b_1 p, \\ \frac{\partial^2 f_8}{\partial x_2 \partial x_7} &= \frac{\partial^2 f_8}{\partial x_7 \partial x_2} = \frac{\partial^2 f_8}{\partial x_4 \partial x_7} = \frac{\partial^2 f_8}{\partial x_7 \partial x_4} = \frac{\partial^2 f_8}{\partial x_6 \partial x_7} \\ &= \frac{\partial^2 f_8}{\partial x_7 \partial x_6} = \frac{\partial^2 f_8}{\partial x_{10} \partial x_7} = \frac{\partial^2 f_8}{\partial x_7 \partial x_{10}} = a_1 c_1, \\ \frac{\partial^2 f_{10}}{\partial x_8 \partial x_9} &= \frac{\partial^2 f_{10}}{\partial x_9 \partial x_8} = a_1 b_1 q. \end{aligned} \tag{8}$$

Additionally,

$$\begin{aligned} \frac{\partial^2 f_3}{\partial x_3 \partial \beta_h} &= \frac{\partial^2 f_3}{\partial \beta_h \partial x_3} = 1, & \frac{\partial^2 f_3}{\partial x_4 \partial \beta_h} &= \frac{\partial^2 f_3}{\partial \beta_h \partial x_4} = \eta_{hh}, \\ \frac{\partial^2 f_3}{\partial x_5 \partial \beta_h} &= \frac{\partial^2 f_3}{\partial \beta_h \partial x_5} = \eta_A, & \frac{\partial^2 f_3}{\partial x_6 \partial \beta_h} &= \frac{\partial^2 f_3}{\partial \beta_h \partial x_6} = \eta_A \eta_{hl}. \end{aligned} \tag{9}$$

Thus, using equations (6), (7), (8), and (9), it can be found that

$$\begin{aligned}
 a = & \frac{a_1 c_1 v_8}{j_{22}} v_8 w_8 a_1 b_1 p \{Q_1 - Q_2\} - \frac{\kappa v_5}{j_{33}} w_5 \left\{ Q_1 \beta^* \left(\frac{j_{55}}{\kappa} + \eta_A \right) - \frac{j_{55}}{\kappa} w_8 a_1 b_1 p \right\} \\
 & + \frac{\varepsilon_1 \kappa v_6 + j_{34} v_3 + a_1 c_1 v_8}{j_{44}} w_5 w_8 a_1 b_1 p \\
 & \left\{ Q_2 + \frac{j_{55}}{\kappa} \right\} - w_5 w_8 \varepsilon_2 a_1 b_1 p \left\{ v_5 - \frac{(\beta^* \eta_A \eta_{hl} v_3 + \phi_3 v_5 + a_1 c_1 v_8)}{j_{66}} \right\} \\
 & - \mu_r v_{10} w_8 \left(\frac{a_1 b_1 p}{j_{22}} w_8 + w_{10} \right) - v_{10} w_8 w_{10} a_1 b_1 q
 \end{aligned} \tag{10}$$

and

$$b = \frac{(\delta_A + \mu_h + \eta_A)(\delta_A + \mu_h + \eta_{AK})}{(\kappa + \mu_h) \eta_{AK}} v_5 w_5 \tag{11}$$

where

$$\begin{aligned}
 Q_1 &= \frac{(j_{12} w_2 - \beta^* w_3 + j_{15} w_5 - a_1 b_1 w_8)}{\mu_h}, \\
 Q_2 &= \frac{\beta^* w_5}{j_{22}} \left(\frac{j_{55}}{\kappa} + \eta_A \right).
 \end{aligned}$$

It is clear from equation 11 that the bifurcation coefficient, b , is automatically positive. Thus, it follows from Theorem 4.1 in [31] that the the HIV-VL co-infection model will undergo backward bifurcation if the bifurcation coefficient, a , given by equation 10, is positive.

3.3 Sensitivity analysis

In this section, sensitivity indices of \mathcal{R}_0 with respect to the parameters are calculated, as shown in Table 2, using the formula, where y is the model parameter, following the technique described in [36, 37]. These indices show how important each parameter is to the disease transmission. Since $\mathcal{R}_0 = \max\{\mathcal{R}_{0l}, \mathcal{R}_{0h}\}$, we obtained the sensitivity indices of \mathcal{R}_{0l} and \mathcal{R}_{0h} separately (see Appendix B).

Table 2 Sensitivity indices table

Parameter symbol	Sensitivity indices
\mathcal{R}_{0h}	Basic reproduction number of VL
c_1	+ve
b_1	+ve
a_1	+ve
ϕ_1	-ve
μ_r	-ve
μ_5	-ve
δ_l	-ve
\mathcal{R}_{0l}	Basic reproduction number of HIV
β_h	+ve
η_a	+ve
k	-ve
δ_a	-ve
μ_h	-ve

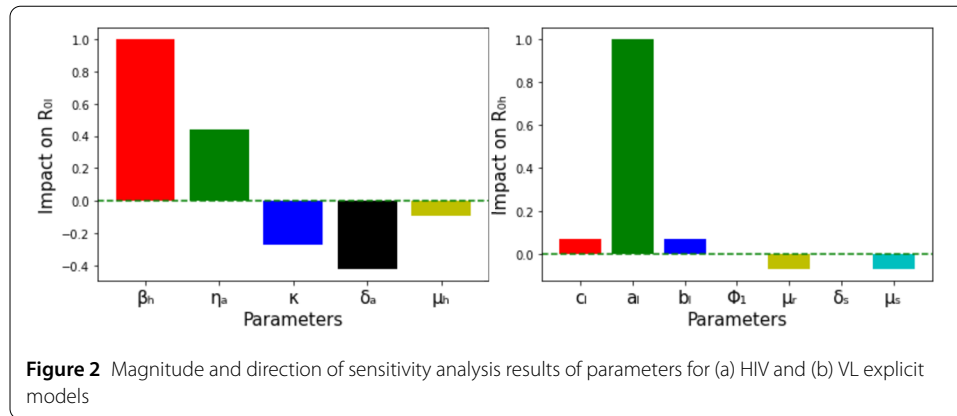


Figure 2 Magnitude and direction of sensitivity analysis results of parameters for (a) HIV and (b) VL explicit models

Table 3 Parameter values of the VL–HIV co-infection model

Parameter	Value day ⁻¹	Source
Λ_h	0.03	Assumed
Λ_s	$0.2999 \times N_s$	[38]
Λ_r	$0.0073 \times N_r$	[5]
μ_h	0.0000395	Assumed
μ_s	0.189	[38]
μ_r	0.000274	[5]
a_l	0.29	Assumed
b_l	varies	Assumed
c_l	0.0714	[7]
ϕ_1, ϕ_2, ϕ_3	varies	Assumed
δ_l	0.011	[39]
δ_A	0.000913	[40]
β_h	varies	Assumed
κ	0.0005	Assumed
$\eta_{hh}, \eta_{A_r}, \eta_{hl}$	1.4, 1.5, 1.001	Assumed
$\varepsilon_1, \varepsilon_2, \tau$	1.002, 0.04, 1.001	Assumed

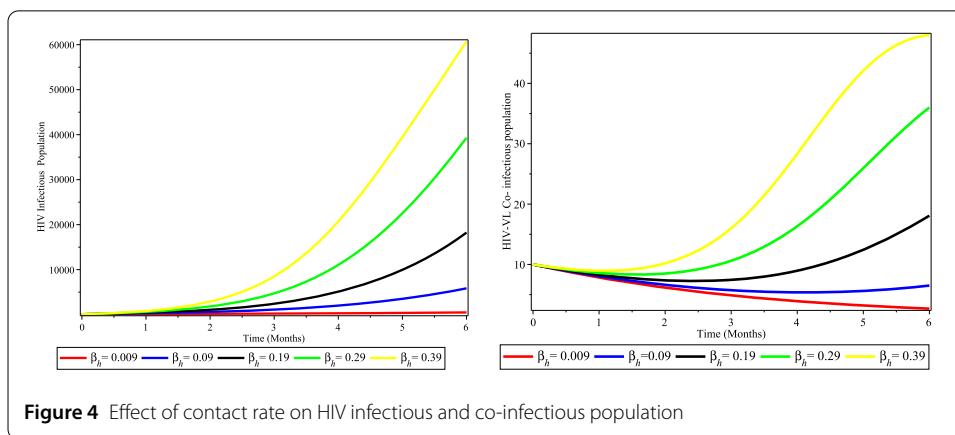
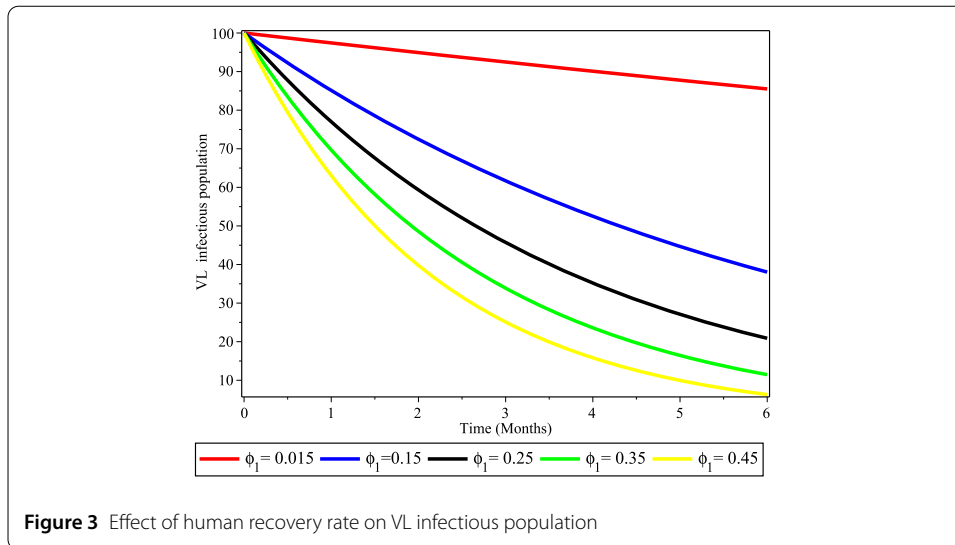
From Fig. 2 and Table 2, we have the following statements. If the sensitivity index is positive, then the reproduction number increases along with increasing value of the parameter. That means that positive index parameters have a power of expanding the disease if their value increases. On the other hand, if the sensitivity index is negative, then reproduction decreases with the increasing value of the parameter. This also mean that negative index parameters have a power of reducing the burden of the disease in the community as their value increases. From this policy makers and stakeholders are expected to act accordingly in combating VL infection, HIV infection, and their co-infection from the community.

4 Numerical simulation

In this section, we use numerical simulations to support the analytical results previously established. We used Maple 18 to show the effect of some parameters in the expansion as well as for the control of HIV only, VL only, and co-infection of HIV and VL. We used parameter values in Table 3 for simulation purpose.

4.1 Effect of human recovery rate (ϕ_1) on VL infectious population

In Fig. 3, we investigated the effect of ϕ_1 in reducing VL-only infectious population by maintaining the other parameters constant. The figure reflects that when the values of ϕ_1 increase, the number of VL only infectious population is diminished. Therefore, we should



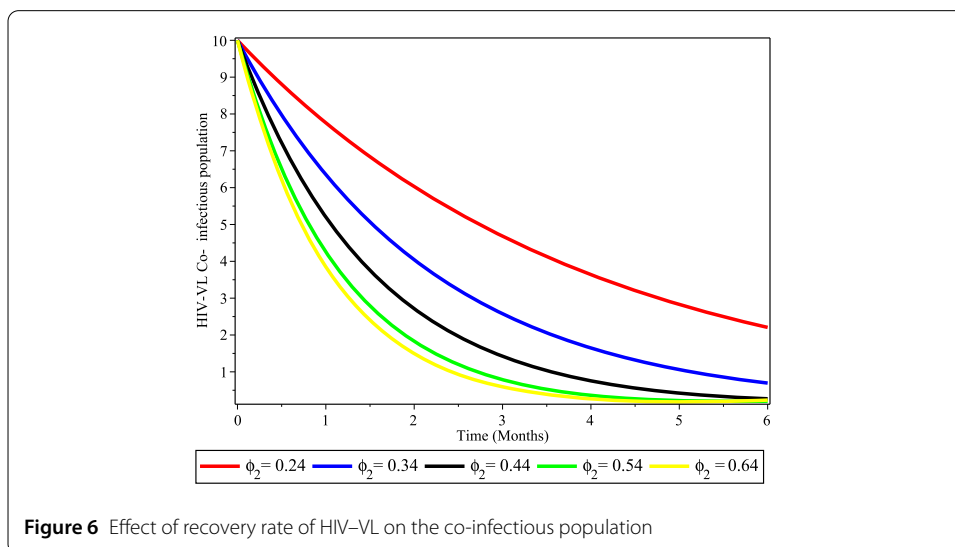
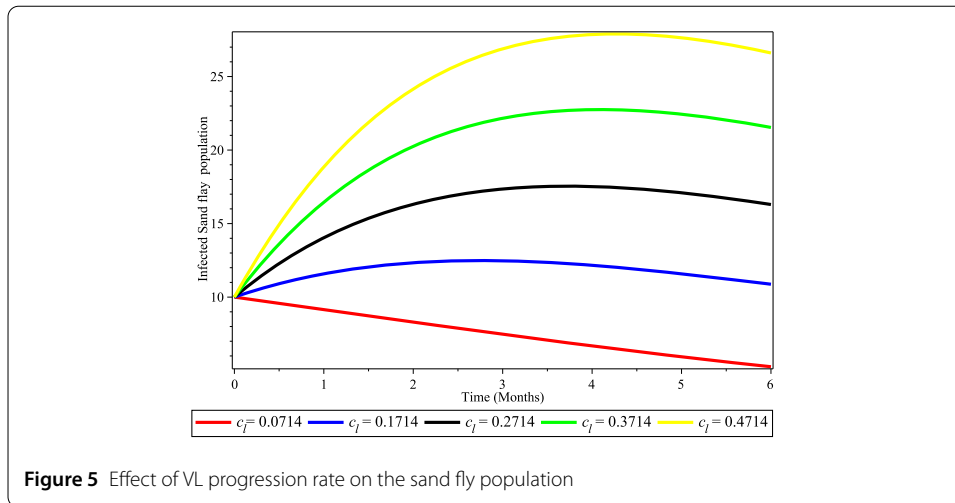
focus on improving recovery rates either by treating infected populations or by increasing the levels of individuals’ immunity to VL disease in the population. Government policy makers should take this into account as a mitigation strategy.

4.2 Effect of effective contact rate (β_h) on HIV infectious and co-infectious population

In this section, we examine the influence of effective contact rate β_h on HIV infectious and HIV–VL co-infectious population. Figure 4 reflects that as the value of contact rate of β_h is increased, the HIV infectious and HIV–VL co-infectious population is increased, which leads to the increased expansion of co-infection of HIV and VL. Consequently, to control HIV infected and co-infection of HIV and VL, decreasing the contact rate of β_h is significant. Therefore, stakeholders need to focus on reducing the contact rate of HIV infectious by using an appropriate method of prevention mechanism to bring down the expansion of co-infection in the community.

4.3 Effect of VL progression rate (c_l) on human and sand fly population

Figure 5 shows the effect of VL progression rate on humans and sand fly population. It reveals that as the VL in humans and sand flies population increases, the infection of pop-



ulation by VL also grows up. Therefore, it is advisable to use treated bed net, chemical techniques to reduce the expansion. This is also another good control strategy to reduce VL infection.

4.4 Effect of recovery rate of HIV-VL (ϕ_2) on the co-infectious population

In this section, we investigate the effect of recovery rate of HIV and VL (ϕ_2) on the co-infectious population. As we clarified in the model description, due to treatment or other mechanisms, the co-infectious population recovers from VL only diseases with their own probability and join the recovered compartment. Therefore, Fig. 6 shows that increasing the rate of recovery of the co-infectious population has a great advantage in reducing VL diseases in the population.

4.5 Effect of VL progression rate in the sand fly reservoir population

Figure 7 shows the effect of VL progression rate on the sand fly reservoir population. It illustrates that as the reservoir increases around the sand fly population, the infection of these reservoirs also increases. From this we can understand that it is important to remove

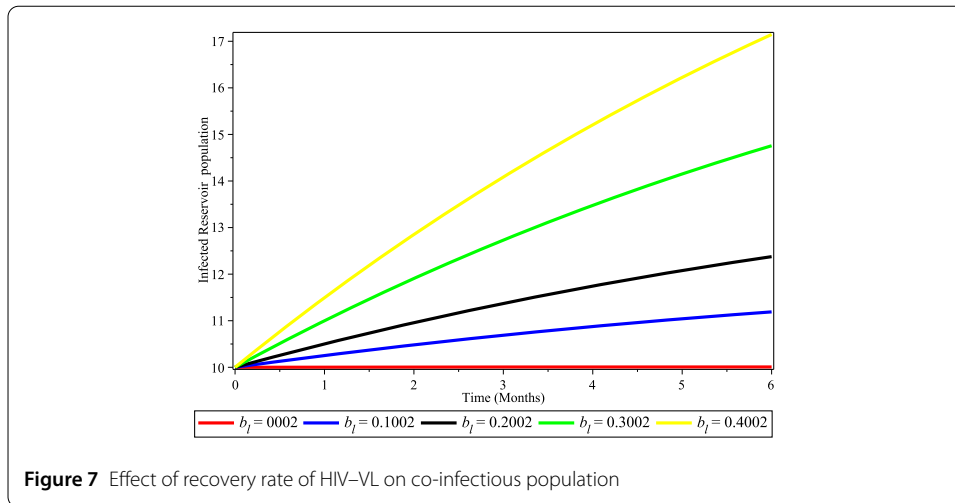


Figure 7 Effect of recovery rate of HIV-VL on co-infectious population

reservoirs from the system to reduce the number of infected reservoirs and infected sand flies. This gives a good control strategy against the disease.

5 Results and conclusions

We developed a transmission dynamics model for VL–HIV co-infection, and the population is subdivided into ten compartments. Before starting the qualitative analysis of the model, we proved the existence of a region where the model is mathematically and epidemiologically well posed. Basic reproduction numbers, disease-free equilibrium, endemic equilibrium, and stability analysis of equilibrium points were analyzed. Numerically, we experimented on the effect of basic parameters in the expansion or control of VL only, HIV only, and their co-infection. From the result, we conclude that an increase in the rate of VL recovery (ϕ_1) contributes greatly to reducing VL infectious individuals in the community. Similarly, increasing the recovery rate for VL-HIV co-infection (ϕ_2) contributes to the reduction of co-infection in the population. Also it is important to remove reservoirs (c_1) from the system so that the number of infected reservoirs and infected sand flies is reduced. Reducing the contact rate β_h is significant in bringing down the number of HIV and VL–HIV co-infected infectious population. The rate of recovery for co-infection also has an influence on dropping co-infectious population if its value has been improved. Therefore, stakeholders should focus on the above basic parameters by using an appropriate method of prevention mechanism to reduce the expansion of infection in VL only, HIV only, and VL–HIV co-infection in the community.

Appendix A: Theorems

Theorem ([41]) For the system

$$\begin{cases} \frac{dX}{dt} = F(X, Z), \\ \frac{dZ}{dt} = G(X, Z), G(X, 0) = 0, \end{cases} \tag{12}$$

where the components of the column vector $X \in R^n$ denote the uninfected populations and $Z \in R^m$ denotes the infected population. $E_0 = (X^*, 0)$ represents the disease-free equilibrium

of this system. E_0 is globally asymptotically stable equilibrium for the model if it satisfies conditions (\mathcal{H}_1) and (\mathcal{H}_2) :

(\mathcal{H}_1) For $\frac{dX}{dt} = F(X, 0), X^*$ is globally asymptotically stable.

(\mathcal{H}_2) $\frac{dZ}{dt} = D_Z G(X^*, 0)Z - \hat{G}(X, Z), \hat{G}(X, Z) \geq 0$ for all $(X, Z) \in \Omega,$

where $D_Z G(X^*, 0)$ is the Jacobian of $G(X, Z)$ taken at the infected population and evaluated at $(X^*, 0).$

Theorem (Castillo-Chavez & Song [31]) *Let us consider the general system of ODEs with a parameter ϕ :*

$$\frac{dx}{dt} = f(x, \phi), \quad f : R^n \times R \longrightarrow R^n, f \in C^2(R^n \times R), \tag{13}$$

where $x = 0$ is an equilibrium point for the system in Eq. (18). That is, $f(0, \phi) \equiv 0$ for all $\phi.$ Assume the following:

M₁: $A = D_x f(0, 0) = (\frac{\partial f}{\partial x_j}(0, 0))$ is the linearization matrix of the system given by (18) around the equilibrium 0 with ϕ evaluated at 0. Zero is a simple eigenvalue of A and other eigenvalues of A have negative real parts;

M₂: Matrix A has a nonnegative right eigenvector w and a left eigenvector v corresponding to the zero eigenvalue. Let f_k be the k th component of f and

$$a = \sum_{k,i,j=1}^n v_k w_i w_j \frac{\partial^2 f_k}{\partial x_i \partial x_j}(0, 0), \quad b = \sum_{k,i=1}^n v_k w_i \frac{\partial^2 f_k}{\partial x_i \partial \phi}(0, 0).$$

The local dynamics of (21) around 0 are totally determined by a and $b.$ If $a < 0$ and $b > 0,$ then the bifurcation is forward; if $a > 0$ and $b > 0,$ then the bifurcation is backward. Using this approach, the following result may be obtained.

Appendix B: Sensitivity of parameters

The sensitivity indices of \mathcal{R}_{0l} and \mathcal{R}_{0h} are given as follows:

$$\begin{aligned} \mathcal{R}_{0l} &= \frac{\beta_h(\delta_A + \mu_h + \eta_A \kappa)}{(\kappa + \mu_h)(\delta_A + \mu_h)}, \\ \mathcal{R}_{0h} &= \sqrt{\frac{a_1 c_l (\mu_r a_l b_l p + a_l b_l q (\phi_1 + \delta_l + \mu_h))}{\mu_s \mu_r (\phi_1 + \delta_l + \mu_h)}}, \\ \left\{ \begin{aligned} \Lambda_{c_1}^{\mathcal{R}_{0h}} &= \frac{\mathcal{R}_{0h}}{\partial c_1} \times \frac{c_1}{\mathcal{R}_{0h}} = \frac{1}{2} \frac{a_l^2 b_l (\mu_r p + q \delta_l + q \mu_h + q \phi_1)}{\mu_s \mu_r (\phi_1 + \delta_l + \mu_h) \sqrt{\frac{a_1^2 c_l b_l (\mu_r p + q \delta_l + q \mu_h + q \phi_1)}{\mu_s \mu_r (\phi_1 + \delta_l + \mu_h)}}} > 0, \\ \Lambda_{b_1}^{\mathcal{R}_{0h}} &= \frac{\mathcal{R}_{0h}}{\partial b_1} \times \frac{b_1}{\mathcal{R}_{0h}} = c_l > 0, \\ \Lambda_{a_1}^{\mathcal{R}_{0h}} &= \frac{\mathcal{R}_{0h}}{\partial a_1} \times \frac{a_1}{\mathcal{R}_{0h}} = \sqrt{\frac{a_1 c_l (\mu_r a_l b_l p + a_l b_l q (\phi_1 + \delta_l + \mu_h))}{\mu_s \mu_r (\phi_1 + \delta_l + \mu_h)}} > 0, \\ \Lambda_{\phi_1}^{\mathcal{R}_{0h}} &= \frac{\partial \mathcal{R}_{0h}}{\partial \phi_1} \times \frac{\phi_1}{\mathcal{R}_{0h}} = -\frac{\phi_1 \mu_r c_l p}{(\mu_r p + q \delta_l + q \mu_h + q \phi_1)(\phi_1 + \delta_l + \mu_h)} < 0, \\ \Lambda_{\mu_r}^{\mathcal{R}_{0h}} &= \frac{\partial \mathcal{R}_{0h}}{\partial \mu_r} \times \frac{\mu_r}{\mathcal{R}_{0h}} = -\frac{q c_l (\phi_1 + \delta_l + \mu_h)}{\mu_r p + q \delta_l + q \mu_h + q \phi_1} < 0, \\ \Lambda_{\delta_l}^{\mathcal{R}_{0h}} &= \frac{\partial \mathcal{R}_{0h}}{\partial \delta_l} \times \frac{\delta_l}{\mathcal{R}_{0h}} = -\frac{\delta_l \mu_r c_l p}{(\mu_r p + q \delta_l + q \mu_h + q \phi_1)(\phi_1 + \delta_l + \mu_h)} < 0, \\ \Lambda_{\mu_s}^{\mathcal{R}_{0h}} &= \frac{\partial \mathcal{R}_{0h}}{\partial \mu_s} \times \frac{\mu_s}{\mathcal{R}_{0h}} = -c_l < 0, \end{aligned} \right. \end{aligned}$$

$$\begin{cases} \Lambda_{\beta_h}^{\mathfrak{N}l} = \frac{\partial \mathfrak{N}l}{\partial \beta_h} \times \frac{\beta_h}{\mathfrak{N}l} = 1 > 0, \\ \Lambda_{\eta_a}^{\mathfrak{N}l} = \frac{\partial \mathfrak{N}l}{\partial \eta_a} \times \frac{\eta_a}{\mathfrak{N}l} = \frac{\eta_a k}{\eta_a k + \delta_a + \mu_h} > 0, \\ \Lambda_k^{\mathfrak{N}l} = \frac{\partial \mathfrak{N}l}{\partial k} \times \frac{k}{\mathfrak{N}l} = -\frac{k(-\eta_a \mu_h + \delta_a + \mu_h)}{(\eta_a k + \delta_a + \mu_h)(k + \mu_h)} < 0, \\ \Lambda_{\delta_a}^{\mathfrak{N}l} = \frac{\partial \mathfrak{N}l}{\partial \delta_a} \times \frac{\delta_a}{\mathfrak{N}l} = -\frac{k \eta_a \delta_a}{(\eta_a k + \delta_a + \mu_h)(\delta_a + \mu_h)} < 0, \\ \Lambda_{\mu_h}^{\mathfrak{N}l} = \frac{\partial \mathfrak{N}l}{\partial \mu_h} \times \frac{\mu_h}{\mathfrak{N}l} = -\frac{\mu_h (k \eta_a (k + \delta_a + 2\mu_h) + (\delta_a + \mu_h)^2)}{(k + \mu_h)(\delta_a + \mu_h)(\eta_a k + \delta_a + \mu_h)} < 0. \end{cases}$$

Acknowledgements

The authors acknowledge the comments of the anonymous reviewers which increased the quality of the paper.

Funding

Not applicable.

Availability of data and materials

The data supporting this deterministic model are from previous published articles.

Competing interests

The authors declare that they have no competing interests.

Authors' contributions

ZTM: Conceptualization, model formulation, qualitative model analysis, and drafting of the manuscript. Also he read and approved the final manuscript. HTA: Numerical simulation, finalizing the manuscript, partial qualitative model analysis, rearranging the overall work. Also he read and approved the final manuscript.

Author details

¹Department of Statistics, College of Natural and Computational Sciences, University of Gondar, Gondar, Ethiopia.

²Department of Mathematics, College of Natural and Computational Sciences, University of Gondar, Gondar, Ethiopia.

Publisher's Note

Springer Nature remains neutral with regard to jurisdictional claims in published maps and institutional affiliations.

Received: 29 March 2021 Accepted: 3 September 2021 Published online: 26 September 2021

References

- Tadese, D., Hailu, A., Bekele, F., Belay, S.: An epidemiological study of visceral leishmaniasis in North East Ethiopia using serological and leishmanin skin tests. *PLoS ONE* **14**(12), 225083 (2019)
- Adriaensen, W., Dorlo, T.P.C., Vanham, G., Kestens, L., Kaye, P.M., van Griensven, J.: Immunomodulatory therapy of visceral leishmaniasis in human immunodeficiency virus-coinfected patients. *Front. Immunol.* **8**, 1943 (2018)
- Kone, A.K., Niaré, D.S., Piarroux, M., Izri, A., Marty, P., Laurens, M.B., Piarroux, R., Thera, M.A., Doumbo, O.K.: Visceral leishmaniasis in West Africa: clinical characteristics, vectors, and reservoirs. *J. Parasitol. Res.* **2019**, Article ID 9282690 (2019)
- Monge-Maillo, B., Norman, F.F., Cruz, I., Alvar, J., Lopez-Velez, R.: Visceral leishmaniasis and HIV coinfection in the Mediterranean region. *PLoS Negl. Trop. Dis.* **8**(8), e3021 (2014)
- Elmojtaba, I.M.: Mathematical model for the dynamics of visceral leishmaniasis–malaria co-infection. *Math. Methods Appl. Sci.* **39**(15), 4334–4353 (2016)
- Lindoso, J.A.L., Moreira, C.H.V., Cunha, M.A., Queiroz, I.T.: Visceral leishmaniasis and HIV coinfection: current perspectives. *HIV/AIDS (Auckl.)* **10**, 193 (2018)
- Lainson, R., Ryan, L., Shaw, J.J.: Infective stages of leishmania in the sandfly vector and some observations on the mechanism of transmission. *Mem. Inst. Oswaldo Cruz* **82**(3), 421–424 (1987)
- Roeger, L.-I.W., Feng, Z., Castillo-Chavez, C.: Modeling TB and HIV co-infections. *Math. Biosci. Eng.* **6**(4), 815 (2009)
- Aldila, D., et al.: Mathematical model for HIV spreads control program with art treatment. *J. Phys. Conf. Ser.* **974**, 012035 (2018)
- Sweileh, W.M.: Global research output on HIV/AIDS–related medication adherence from 1980 to 2017. *BMC Health Serv. Res.* **18**(1), 1–13 (2018)
- World Health Organization: Fifth Consultative Meeting on Leishmania/HIV Coinfection, Addis Ababa, Ethiopia. World Health Organization, Geneva (2007)
- World Health Organization: Leishmaniasis and HIV Coinfection. Geneva. World Health Organization, Switzerland (2014)
- Shiri, B., Baleanu, D.: Numerical solution of some fractional dynamical systems in medicine involving non-singular kernel with vector order. *Results Nonlinear Anal.* **2**(4), 160–168 (2019)
- Liancheng, W.A.N.G., Xiaoqin, W.U.: Stability and Hopf bifurcation for an SEIR epidemic model with delay. *Adv. Theory Nonlinear Anal. Appl.* **2**(3), 113–127 (2018)
- Waziri, A.S., Massawe, E.S., Makinde, O.D.: Mathematical modelling of HIV/AIDS dynamics with treatment and vertical transmission. *Appl. Math.* **2**(3), 77–89 (2012)

16. Mastroberardino, A., Cheng, Y., Abdelrazec, A., Liu, H.: Mathematical modeling of the HIV/AIDS epidemic in Cuba. *Int. J. Biomath.* **8**(04), 1550047 (2015)
17. Omondi, E.O., Mbogo, R.W., Luboobi, L.S.: A mathematical modelling study of HIV infection in two heterosexual age groups in Kenya. *Infect. Dis. Model.* **4**, 83–98 (2019)
18. Sohaib, M., et al.: Mathematical modeling and numerical simulation of HIV infection model. *Results Appl. Math.* **7**, 100118 (2020)
19. Ribas, L.M., Zaher, V.L., Shimozako, H.J., Massad, E.: Estimating the optimal control of zoonotic visceral leishmaniasis by the use of a mathematical model. *Sci. World J.* **2013**, Article ID 810380 (2013)
20. Zou, L., Chen, J., Ruan, S.: Modeling and analyzing the transmission dynamics of visceral leishmaniasis. *Math. Biosci. Eng.* **14**(5–6), 1585 (2017)
21. Agyingi, E., Wiandt, T.: Analysis of a model of leishmaniasis with multiple time lags in all populations. *Math. Comput. Appl.* **24**(2), 63 (2019)
22. Song, Y., Zhang, T., Li, H., Wang, K., Lu, X.: Mathematical model analysis and simulation of visceral leishmaniasis, Kashgar, Xinjiang, 2004–2016. *Complexity* **2020**, Article ID 5049825 (2020)
23. Elmojtaba, I.M., Mugisha, J.Y.T., Hashim, M.H.A.: Vaccination model for visceral leishmaniasis with infective immigrants. *Math. Methods Appl. Sci.* **36**(2), 216–226 (2013)
24. Elmojtaba, I.M., Mugisha, J.Y.T., Hashim, M.H.A.: Modelling the role of cross-immunity between two different strains of leishmania. *Nonlinear Anal., Real World Appl.* **11**(3), 2175–2189 (2010)
25. Elmojtaba, I.M., Mugisha, J.Y.T., Hashim, M.H.A.: Mathematical analysis of the dynamics of visceral leishmaniasis in the Sudan. *Appl. Math. Comput.* **217**(6), 2567–2578 (2010)
26. Mukandavire, Z., Gumel, A.B., Garira, W., Tchuenche, J.M.: Mathematical analysis of a model for HIV-malaria co-infection. *Math. Biosci. Eng.* **6**(2), 333 (2009)
27. Hussaini, N., Lubuma, J.M.S., Barley, K., Gumel, A.B.: Mathematical analysis of a model for AVL-HIV co-endemicity. *Math. Biosci.* **271**, 80–95 (2016)
28. Vandermeer, J.H., Goldberg, D.E.: *Population Ecology: First Principles*. Princeton University Press, Princeton (2013)
29. Van den Driessche, P., Watmough, J.: Reproduction numbers and sub-threshold endemic equilibria for compartmental models of disease transmission. *Math. Biosci.* **180**(1–2), 29–48 (2002)
30. Alemneh, H.T.: A co-infection model of Dengue and leptospirosis diseases. *Adv. Differ. Equ.* **2020**(1), 1 (2020)
31. Castillo-Chavez, C., Song, B.: Dynamical models of tuberculosis and their applications. *Math. Biosci. Eng.* **1**(2), 361–404 (2004)
32. Carr, J.: *Applications of Centre Manifold Theory*. Springer, Berlin (1981)
33. Berhe, H.W., Makinde, O.D., Theuri, D.M.: Co-dynamics of measles and dysentery diarrhea diseases with optimal control and cost-effectiveness analysis. *Appl. Math. Comput.* **347**, 903–921 (2019)
34. Melese, Z.T., Mwalili, S.M., Orwa, G.O.: Threshold dynamics of the transmission of antibiotic-resistant infections. *Biosystems* **171**, 80–92 (2018)
35. Dushoff, J., Huang, W., Castillo-Chavez, C.: Backwards bifurcations and catastrophe in simple models of fatal diseases. *J. Math. Biol.* **36**(3), 227–248 (1998)
36. Blower, S.M., Dowlatabadi, H.: Sensitivity and uncertainty analysis of complex models of disease transmission: an HIV model, as an example. *Int. Stat. Rev.* **62**(2), 229–243 (1994)
37. Alemneh, H.T., Alemu, N.Y.: Mathematical modeling with optimal control analysis of social media addiction. *Infect. Dis. Model.* **6**, 405–419 (2021)
38. Kasap, O.E., Bulent, A.: Comparative demography of the sand fly phlebotomus papatasi (diptera: psychodidae) at constant temperatures. *J. Vector Ecol.* **31**(2), 378–385 (2006)
39. Sundar, S., Lockwood, D.N.J., Agrawal, G., Rai, M., Makharia, M.K., Murray, H.W.: Treatment of Indian visceral leishmaniasis with single or daily infusions of low dose liposomal amphotericin b: randomised trialcommentary: cost and resistance remain issues. *BMJ, Br. Med. J.* **323**(7310), 419–422 (2001)
40. Mukandavire, Z., Garira, W.: Sex-structured HIV/AIDS model to analyse the effects of condom use with application to Zimbabwe. *J. Math. Biol.* **54**(5), 669–699 (2007)
41. Castillo-Chavez, C., Blower, S., van den Driessche, P., Kirschner, D., Yakubu, A.-A.: *Mathematical Approaches for Emerging and Reemerging Infectious Diseases: Models, Methods, and Theory*. Springer, New York (2002)

Submit your manuscript to a SpringerOpen[®] journal and benefit from:

- Convenient online submission
- Rigorous peer review
- Open access: articles freely available online
- High visibility within the field
- Retaining the copyright to your article

Submit your next manuscript at ► [springeropen.com](https://www.springeropen.com)